

Realizing Wireless Communication through Software-defined HyperSurface Environments

Christos Liaskos*, Shuai Nie[†], Ageliki Tsioliaridou*, Andreas Pitsillides[‡], Sotiris Ioannidis*, and Ian Akyildiz^{†‡}

*Foundation for Research and Technology - Hellas (FORTH)

Emails: {cliaskos,atsiolia,sotiris}@ics.forth.gr

[†]Georgia Institute of Technology, School of Electrical and Computer Engineering

Emails: {shuainie, ian}@ece.gatech.edu

[‡]University of Cyprus, Computer Science Department

Email: Andreas.Pitsillides@ucy.ac.cy

Abstract—Wireless communication environments are unaware of the ongoing data exchange efforts within them. Moreover, their effect on the communication quality is intractable in all but the simplest cases. The present work proposes a new paradigm, where indoor scattering becomes software-defined and, subsequently, optimizable across wide frequency ranges. Moreover, the controlled scattering can surpass natural behavior, exemplary overriding Snell’s law, reflecting waves towards any custom angle (including negative ones). Thus, path loss and multi-path fading effects can be controlled and mitigated. The core technology of this new paradigm are metasurfaces, planar artificial structures whose effect on impinging electromagnetic waves is fully defined by their macro-structure. The present study contributes the software-programmable wireless environment model, consisting of several HyperSurface tiles controlled by a central, environment configuration server. HyperSurfaces are a novel class of metasurfaces whose structure and, hence, electromagnetic behavior can be altered and controlled via a software interface. Multiple networked tiles coat indoor objects, allowing fine-grained, customizable reflection, absorption or polarization overall. A central server calculates and deploys the optimal electromagnetic interaction per tile, to the benefit of communicating devices. Realistic simulations using full 3D ray-tracing demonstrate the groundbreaking potential of the proposed approach in 2.4GHz and 60GHz frequencies.

Index Terms—Wireless Environment, Communication-awareness, Indoor, Millimeter wave, Software control, Metasurfaces.

I. INTRODUCTION

Recent years have witnessed a tremendous increase in the efficiency of wireless communications. Multiple techniques have been developed to tackle the stochastic nature of the wireless channel, in an effort to fully adapt to its wide fluctuations. Indoor environments have attracted special attention, since multi-path fading accentuates due to the presence of multiple scatterers in a confined space. In such cases, techniques such as MIMO, beamforming, adaptive modulation and encoding have enabled wireless devices to rapidly adapt to the time-variant, unpredictable channel state [1]. The present work opens an unexplored research path: making the wireless environment fully controllable via software, enabling the optimization of major propagation factors between wireless devices. Thus,

effects such as path loss and multi-path fading become controllable and mitigate-able.

In order to understand the potential of exerting control over an environment, we first need to define its composition and its natural behavior. Indoor environments, which constitute the focus of the present work, comprise two or more communicating devices—such as laptops, mobile phones, access points, base stations etc.—and any object found in a domestic or work space that can influence their communication. At lower frequencies, walls, ceilings, floors, doors and sizable furniture act as electromagnetic (EM) wave scatterers, creating multiple paths between communicating end-points, especially in non-line-of-sight (NLOS) areas. At higher frequencies, such as millimeter wave (mm-wave) or terahertz (THz), which are expected to play a major role in upcoming 5G communications [5], even small objects act as substantial scatterers. Furthermore, ultra-small wavelengths translate to considerable Doppler shift even at pedestrian speed [5]. These factors, coupled with the natural ambient dissipation of power due to free space losses, lead to undermined NLOS performance at 2–5 GHz and inability for NLOS communications at 60 GHz and beyond [5].

Existing proposals for multi-path and path loss mitigation can be classified as i) device-oriented, and ii) retransmitter-oriented. Device-oriented methods include massive MIMO deployments in communicating devices, to make constructive use of the multi-path phenomena [6]. Additionally, beamforming seeks to adaptively align the direction of wireless transmissions in order to avoid redundant free space losses [7], [8]. Additional schemes include the on-the-fly selection of the modulation and encoding scheme that offers the best bit error rate (BER) under the current channel conditions [9]. Retransmission-oriented solutions advocate for the placement of amplifiers in key-positions within the indoor environment. Retransmitters can be either passive or active: Passive retransmitters are essentially conductive structures akin to antenna plates [10]. They passively reflect energy from and towards fixed directions, without tunability. Active retransmitters are powered electronic devices that amplify and re-transmit received signals within a given frequency band. Essentially, they attempt to combat power loss by diffusing more power within the environment. In mm-wave

frequencies and beyond, retransmitters must be placed in line-of-sight (LOS) among each other, in an effort to eliminate NLOS areas within a floor plan. Device-to-device networking can also act as a retransmission solution for specific protocols and a limited capacity of served users [11]. The overviewed solutions have a common trait: They constitute device-side approaches, which treat the environment as an uncontrollable factor that does not participate into the communication process.

Metasurfaces are the core technology for introducing programmatically controlled wireless environments [12]–[14]. They constitute the outcome of a research direction in Physics interested in creating (rather than searching for) materials with required EM properties. In their earlier iterations, they comprised a metallic pattern, called *meta-atom*, periodically repeated over a Silicon substrate, as shown in Fig. 2. The macroscopic EM behavior of a metasurface is fully defined by the meta-atom form. A certain pattern may fully absorb all impinging EM waves from a given direction of arrival (DoA), while another may fully reflect a given DoA towards another, at a negative reflection angle. Notably, metasurfaces (and their 3D counterpart, the metamaterials) offer a superset of EM behaviors with regard to regular materials. Lens functionality (concentration of reflections towards a given point rather than ambient dispersal) and negative refraction/reflection indexes are but some of the exotic EM capabilities they can exhibit [15]. Dynamic meta-atom designs allow for dynamic metasurfaces, as shown in Fig. 2. Such designs include tunable factors, such as CMOS switches or Micro Electro-Mechanical Switches (MEMS) that can alter their state—and the EM behavior of the metasurface—via an external bias [15]. The bias is commonly electronic, but thermal, light-based and mechanical approaches have been studied as well [15]. Thus, multi-functional metasurfaces, that can switch from one EM behavior to another (e.g., from absorbing to custom steering) are enabled. Finally, a very strong trait is that there is no known limitation to the operating metasurface frequency, which can be at the *mm*-wave and *THz* bands [16].

The methodology proposed by the present study is to coat objects of EM significance within an indoor environment with a novel class of software-controlled metasurfaces. The study defines a unit of this metasurface class, called *HyperSurface tile*. A HyperSurface tile is a planar, rectangular structure that incorporates networked hardware control elements and adaptive meta-atom metasurfaces. Following a well-defined programming interface, a tile can receive external commands and set the states of its control elements to match the intended EM behavior. The tiles, covering walls, doors, offices, etc., form networks to facilitate the relaying of programmatic commands among them. Moreover, tiles can have environmental sensing and reporting capabilities, facilitating the discovery of communicating devices within the environment. As shown in Fig. 1, a central server can receive incoming tile reports, calculate the optimal configuration per tile, and set the environment in the intended state by sending the corresponding commands. Collaboration with existing systems (e.g., localization services and Cloud computing), constitutes a strong aspect of the

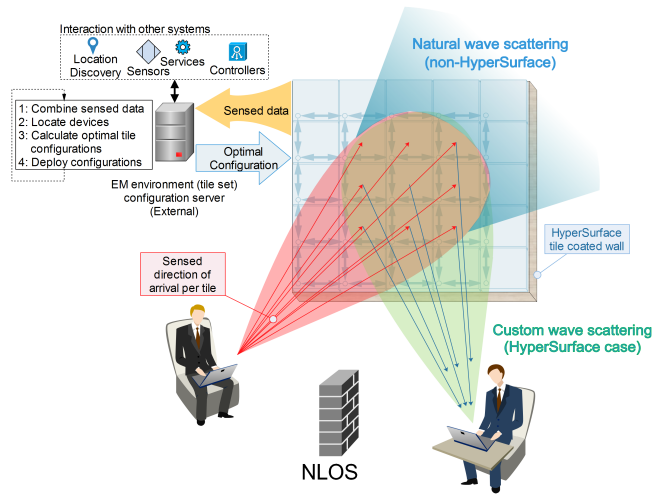


Fig. 1: The proposed workflow involving HyperSurface tile-coated environmental objects. The EM scattering is tailored to the needs of the communication link under optimization. Unnatural EM scattering, such as lens-like EM focus and negative reflection angles can be employed to mitigate path loss and multi-path phenomena, especially in challenging NLOS cases.

proposed approach, given that it enables the incorporation of the EM behavior of materials in smart control loops.

The present study contributes the first model to describe programmable wireless indoor environments, detailing their hardware, networking and software components. The model includes the way for translating EM metasurface functionalities to reusable software functions, bridging physics and informatics. Moreover, the protocol specifications and programming interfaces for interacting with tiles for communication purposes are outlined. The practical procedure for deploying programmable EM environments to mm-wave indoor communication is detailed. The potential of programmable environments is evaluated via full 3D ray tracing in 2.4 and 60 GHz cases, demonstrating their ground-breaking potential in mitigating path loss and multi-path fading effects. The study also presents a way of modifying common ray-tracers to enable their use in programmable EM environment simulations. Uses of the proposed concept in other application domains are also discussed.

The remainder of the text is organized as follows. Prerequisite knowledge on metasurfaces is given in Section II. The HyperSurface-based wireless environment model is given in Section III. Applications to indoor wireless setups are discussed in Section V. Evaluation via ray-tracing-based simulations is presented in Section VI. Finally, the conclusion is given in Section VII.

II. PREREQUISITES

This section provides the necessary background knowledge on metasurfaces, discussing dimensions and composition, operating principles and supported functionalities. The following concise description targets a wireless communications audience, given the topic of the present paper. A more detailed introduction can be found in [17].

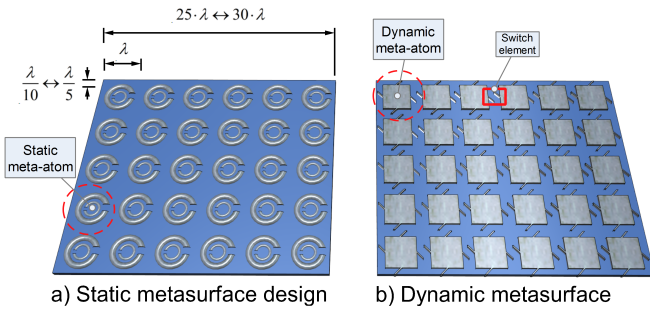


Fig. 2: Split ring resonators (left) constituted a very common type of static metasurfaces, with fixed EM behavior. Novel designs (right) incorporate switch elements (MEMS, CMOS or other) to offer dynamically tunable EM behavior.

A metasurface is a planar, artificial structure which comprises a repeated element, the meta-atom, over a substrate. In most usual compositions, the meta-atom is conductive and the substrate is dielectric. Common choices are copper over silicon, while silver and gold constitute other exemplary conductors [12]. More exotic approaches employ graphene, in order to interact with THz -modulated waves [16]. Metasurfaces are able to control EM waves impinging on them, in a frequency span that depends on the overall dimensions. The size of the meta-atom is comparable to the intended interaction wavelength, λ , with $\lambda/2$ constituting a common choice. The thickness of the metasurface is smaller than the interaction wavelength, ranging between $\lambda/10 \rightarrow \lambda/5$ as a rule of a thumb. Metasurfaces usually comprise several hundreds of meta-atoms, which results into fine-grained control over the EM interaction control. In general, a minimum size of approximately 30×30 meta-atoms is required to yield an intended EM interaction [15].

Figure 2-a illustrates a well-studied metasurface design comprising split-ring resonators as the meta-atom pattern. Such classic designs that rely on a static meta-atom, naturally yield a static interaction with EM waves. The need for dynamic alteration of the EM wave control type has given rise to dynamic metasurfaces, illustrated in Fig. 2-b. Dynamic meta-atoms incorporate phase switching components, such as MEMS or CMOS transistors, which can alter the structure of the meta-atom. Thus, dynamic meta-atoms allow for time-variant EM interaction, while meta-atom alterations may give rise to multi-frequency operation [12]. Phase switching components can also be classified into state-preserving or not. For instance, mechanical switches may retain their state and require powering only for state transitions, while semiconductor switches require power to maintain their state.

The operating principle of metasurfaces is given in Fig. 3. The meta-atoms, and their interconnected switch elements in the dynamic case, act as control factors over the surface currents flowing over the metasurface. The total EM response of the metasurface is then derived as the total emitted field by all surface currents, and can take completely engineered forms, such as the unnatural reflection angle shown in Fig. 3. Engineering the total surface current is a complex process that

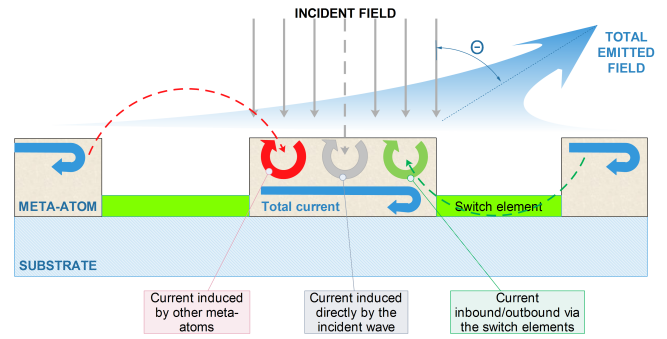


Fig. 3: The principle of metasurface functionality. Incident waves create a well-defined EM response to the unit cells. The cell response is crafted in such a way that the aggregate field follows a metasurface-wide design objective, e.g., reflection towards a custom angle Θ .

must account for currents directly induced over the metasurface by the incident wave, the currents induced in a meta-atom wirelessly by other meta-atoms, as well as the currents flowing inwards or outwards from a meta-atom via the switch elements. A qualitative description of the dynamic metasurface operation can also be given: the meta-atoms can be viewed as either input or output antennas, connected in custom topologies via the switch elements. Impinging waves enter from the input antennas, get routed according to the switch element states, and exit via the output antennas, exemplary achieving customized reflection.

A. State-of-the-art potential and manufacturing approaches

Metasurfaces constitute the state of the art in EM control in terms of capabilities and control granularity. A metasurface can support a wide range of EM interactions, denoted as *functions*. Common function types include [13]:

- Reflection of an impinging wave, with a given direction of arrival, towards a completely custom direction.
- Refraction of EM waves via the metasurface towards any inwards direction. Both the reflection and refraction functions can override the outgoing directions predicted by Snell's law. Reflection and refraction functions will jointly be referred to as wave *steering*.
- Wave absorbing, i.e., ensuring minimal reflected and/or refracted power for impinging waves.
- Wave polarizing, i.e., changing the oscillation orientation of the wave's electric and magnetic field.

Moreover, they can offer additional, advanced functions, such as collimation, resulting from near zero permittivity and permeability response, anisotropic response leading to hyperbolic dispersion relation, giant chirality, arbitrary wavefront shaping and frequency selective filtering [14]. Apart from communications, these traits have been exploited in a variety of applications, e.g., highly efficient energy harvesting photovoltaics, and thermophotovoltaics, ultra-high resolution medical imaging, sensing, quantum optics and military applications [18].

The extended repertoire of EM function types, as well as the exquisite degree of granularity in EM behavior control, sets metasurfaces apart from phased antennas and reflectarrays [8],

[19], which can only support coarse EM steering, e.g., for beamforming applications in wireless devices [7]. Notice that highly fine-grained EM control is required in mm-wave setups, due to the extremely small wavelength [5].

Regarding their manufacturing approaches, metasurfaces are commonly produced as conventional printed circuit boards (PCBs) [20]. The PCB approach has the advantage of relying on a mature, commercially accessible manufacturing technology. The PCB production cost is moderate (indicatively, USD 500 per m^2 [21]). However, the PCB technology is originally intended for integrated circuits with far greater complexity than a metasurface. As described in the context of Fig. 2, a metasurface can be a very simple structure, comprising a set of conductive patches, diodes and conductive power/signal lines. Therefore, large area electronics (LAE) can constitute better manufacturing approaches in terms of ultra low production cost [22], [23]. LAE can be manufactured using conductive ink-based printing methods on flexible and transparent polymer films, and incorporate polymer/organic diodes [24]. Films with metasurface patterns and diodes printed on them can then be placed upon common objects (e.g., glass, doors, walls, desks), which may also act as the dielectric substrate for the metasurface.

III. THE HYPERSURFACE-BASED WIRELESS ENVIRONMENT MODEL

This section details the HyperSurface tile hardware components, the tile inter-networking and the environment control software. A schematic overview is given in Fig. 4 and is detailed below.

The tile hardware. The tile hardware consists of a dynamic metasurface, a set of networked, miniaturized controllers that control the switch elements of the metasurface, and a gateway that provides inter-tile and external connectivity. The controller network has a slave/master relation to the gateway. Via the gateway, the controller network reports its current state and receives commands to alter the state of the switch elements in a robust manner, making the metasurface yield an overall required EM function.

A single controller is a miniaturized, addressable electronic device that can monitor and modify the state of at least one metasurface switch element. The controller design objectives are small size (to avoid significant interference to the EM function of the metasurface), low-cost (to support massive deployments in many tiles), high monitoring and actuation speed (to sustain fast EM reconfigurability of the metasurface), and the ability to create, receive and relay data packets (to enable controller networking).

The avoidance of EM function disruption also refers to the wiring required to connect the controllers to the switch elements and to each other in a grid topology (cf. Fig. 4). Therefore, the total wiring should also be kept low. The grid-networked controller approach is an option that balances wiring length and robustness to node failures. Bus connectivity for the controllers would minimize the required wiring, but would decrease the robustness against node failures. On the other

hand, a star connectivity would offer maximum robustness but would also yield maximum wiring. Notice that future technologies, such as nanonetworking, may enable wireless, computationally-powerful nodes with autonomous, energy harvesting-based power supply [25]. Thus, future tile designs may need no wiring or specific gateways. The setup presented in this study prioritizes cost-effective realizability with present manufacturing capabilities.

At a logical level, a controller is modeled as a finite-state automaton, which reacts to incoming packets or switch element changes by transitioning from one state to another [26]. A UML-standard state diagram should capture three basic controller processes: the data packet handling (including re-routing, consuming packets and sending acknowledgments), the node reporting (reacting to an incoming monitoring directive—monitor request packet—by creating a new monitor data packet), and a fault detection process (either self- or neighbor-failure). The latter is required for robust data routing and for deducing the operational state of the tile as a whole. Regarding the controller addressing, it can be hardwired due to the fixed grid topology.

The tile gateway stands between the tile controller network and the external world. It is incorporated to the tile fabric at a position selected to yield minimal EM interaction concerns (e.g., at the back of the tile). It provides mainstream protocol-compatible data exchange with any other system. Internally, it is connected to at least one controller, while more connections can be used for robust connectivity. Moreover the gateway acts as a power supply bridge for the tile. Limited size (e.g., $\sim cm$) and energy requirements are the only significant constraints. Existing hardware, such as IoT platforms [27], can be employed as tile gateways [27]. The tile gateway may optionally have EM DoA sensing capabilities, to facilitate the location discovery of wireless user devices in the environment.

The tile inter-networking. As tiles are placed over an environmental object, such as a wall, they click together, connecting data and power lines among the tile gateways (cf. Fig. 4). Thus, the tiles form a wired ad hoc network in a grid topology. Once again, existing IoT communication protocols can be readily employed. The same protocol is used for connecting the tile network to any external system. At least one tile—denoted as exit/entry point—has its gateway connect to the environment configuration server, which accumulates sensed data and diffuses EM actuation commands within the tile network. More than one tile can be used as exit/entry points at the same time, for the interest or robust and timely data delivery.

The environment control software. The environment control software is an application programming interface (API) that exists at the configuration server. The API serves as a strong layer of abstraction, hiding the internal complexity of the HyperSurfaces. It offers user-friendly and general purpose access to metasurface functions, without requiring knowledge of the underlying hardware and Physics. It provides software descriptions of metasurface functions, allowing a programmer to customize, deploy or retract them on-demand over tiles with appropriate callbacks. These callbacks have the following

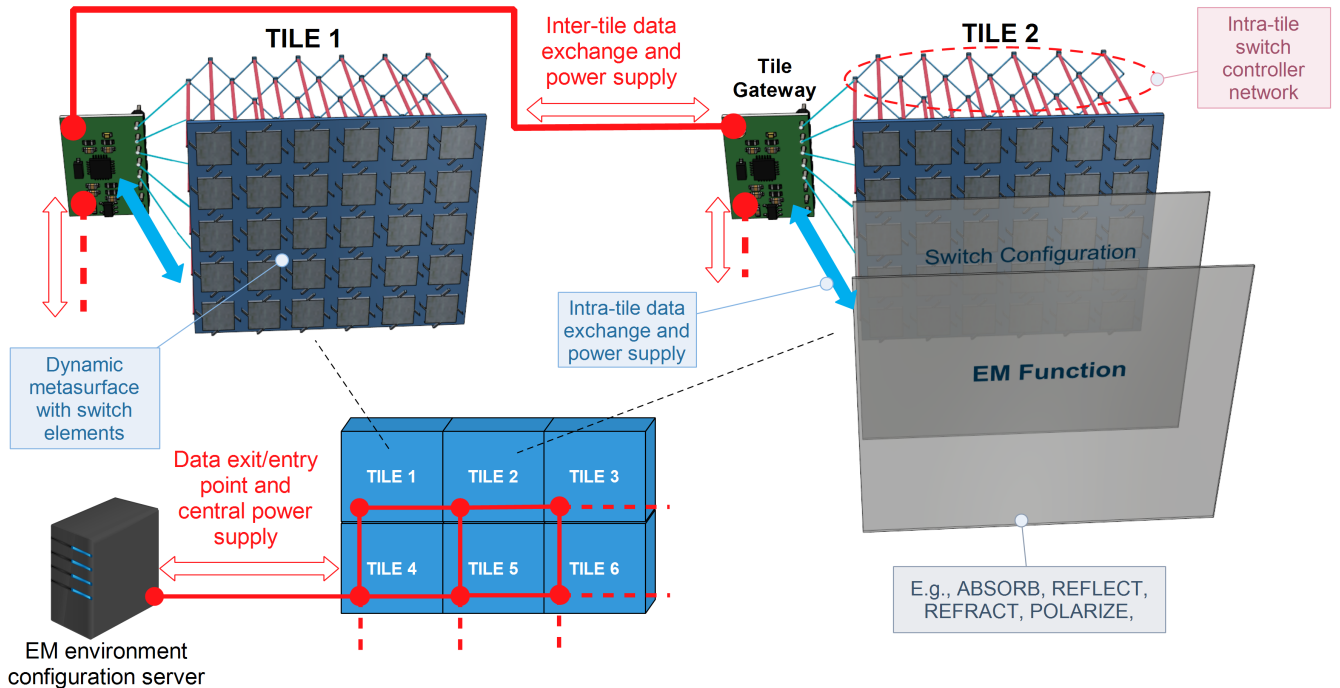


Fig. 4: Illustration of the HyperSurface tile architecture and the tile-enabled wireless environment model.

general form:

```
outcome ← callback(tile_ID, action_type, parameters)
```

The `tile_ID` is the unique address of the intended tile gateway in the inter-tile network (e.g., an IPv6). One EM function per tile is considered here for simplicity. The `action_type` is an identifier denoting the intended function, such as STEER or ABSORB, as described in Section II. Each action type is associated to a set of valid parameters. For instance, STEER commands require: i) an incident DoA, \vec{T} , ii) an intended reflection direction, \vec{O} , and iii) the applicable wavelength, λ , (if more than one are supported). ABSORB commands require no \vec{O} parameter. Notice that metasurface properties can be symmetric: i.e., a STEER(\vec{T}, \vec{O}) can also result into STEER(\vec{O}, \vec{T}) [28].

Once executed at the configuration server, a callback is translated to an appropriate configuration of the switch elements that should be deployed at the intended tile. The configuration is formatted as a data packet that enters the tile network via an entry/exit point, and is routed to the intended tile via the employed inter-tile routing protocol. The intended tile gateway translates the directive according to the controller network communication protocol specifications and diffuses it within the tile. Upon success, it returns an acknowledgment to the configuration server, or an error notification otherwise.

In the general case, the translation of an EM function to a tile switch element configuration is accomplished via a lookup table, populated during the tile design/manufacturing process as follows. Let σ be a single tile configuration, defined as an

array with elements s_{ij} describing the intended switch element state that is overlooked by controller with address i, j in the tile controller network. (One-to-one controller-switch relation is assumed). In the MEMS case, s_{ij} takes binary values, 1 or 0, denoting switch connection or disconnection. Additionally, let Σ be the set of all possible configurations, i.e., $\sigma \in \Sigma$. Let an EM function of type ABSORB from DoA \vec{T} be of interest. Moreover, let $P_{\sigma}(\phi, \theta)$ be the power reflection pattern of the tile (in spherical coordinates), when a wave with DoA \vec{T} impinges upon it and a configuration σ is active. Then, the configuration σ_{best} that best matches the intended function ABSORB(\vec{T}) is defined as:

$$\sigma_{best} \leftarrow \underset{\sigma \in \Sigma}{\operatorname{argmin}} \{ \max_{\phi, \theta} P_{\sigma}(\phi, \theta) \} \quad (1)$$

Existing heuristic optimization processes can solve this optimization problem for all functions of interest in an offline manner [29], using simulations or field measurements on prototypes. The configuration lookup table is thus populated. Finally, we note that analytical results for the EM function-configuration relation exist in the literature for several metasurface designs [29]. In such cases, the analytical results can be employed directly, without the need for lookup tables.

IV. CONTROL ALGORITHM OF HYPERSURFACE

In order to establish communication links between transmitters and receivers, the HyperSurface tiles need to be adaptively selected and optimally controlled to serve the desired receivers. Since in real-world communication scenarios, multiple users

can be present in the same space, it is necessary to discuss the tile distribution and control algorithms.

We start from the case where there is one pair of transmitter and receiver in the environment, as shown in Fig. 5. When the transmitter sends signals, multiple tiles can sense the transmitted signals. According to the location of the receiver sensed by the location discovery system, those tiles will steer their angles to establish reflection paths. Therefore, the signal received at the receiver is a superposition of all signals reflected from various tiles. Among all tiles, only those that can sense the transmitted signals will respond to forwarding requests and tune their angles. On the other hand, in a more complicated case where multiple users are present in the same environment, the tile distribution needs to be optimized. The signals to be received by different users should be orthogonal to each other and are forwarded by different HyperSurface paths.

We assume the transmitted signal is QPSK modulated with symbol $k(t)$, thus in general the received signal in time domain can be expressed as

$$r(t) = k(t) \sum_{i=1}^N a_i e^{-j\theta_i} e^{j2\pi f_c \tau_i} + n(t), \quad (2)$$

where f_c is the central frequency, a_i , θ_i , and τ_i are the attenuation, phase, and delay caused by the reflection paths along HyperSurface tiles of i -th path, and $n(t)$ is the AWGN noise in the channel. We assume there are in total N paths found between the transmitter and receiver. The multipath effects might cause distortion in overall received signal, therefore we need to mitigate the destructive interference and harmonize the phases by controlling the operation of HyperSurface tiles. Specifically, we can formulate it as an optimization problem aimed at maximizing the received power, $P_r^{(j)}$, and the number of tiles of the HyperSurface, $M_{HS}^{(j)}$, for the j^{th} receiver in the network with a total of J users with d_j distance, as follows:

$$\text{Given: } (x_t, y_t, z_t), (x_r^{(j)}, y_r^{(j)}, z_r^{(j)}), \quad (3)$$

$$P_t^{\text{total}}, M_{HS}^{\text{total}} \quad (4)$$

$$\text{Find: } P_t^{(j)}, M_{HS}^{(j)} \quad (5)$$

$$\text{Objective: } \max \sum d_j P_r^{(j)} \quad (6)$$

Subject to:

$$\text{Transmit power allocation: } \sum P_t^{(j)} \leq P_t^{\text{total}} \quad (7)$$

$$\text{HyperSurface tile allocation: } \sum M_{HS}^{(j)} \leq M_{HS}^{\text{total}} \quad (8)$$

$$\text{for all } j \in J \quad (9)$$

In the above optimization problem, (x_t, y_t, z_t) and $(x_r^{(i)}, y_r^{(i)}, z_r^{(i)})$ denote the three-dimensional coordinates of the transmitter and the i^{th} receiver, respectively. Based on the above optimization problem, we can distribute tiles to corresponding users without causing interference or signal distortion.

V. APPLICATIONS TO MM-WAVE INDOOR SETUPS

In mm-wave setups, major factors affect the signal attenuation: i) the increased free space path loss (e.g., $\sim 90\text{dB}$

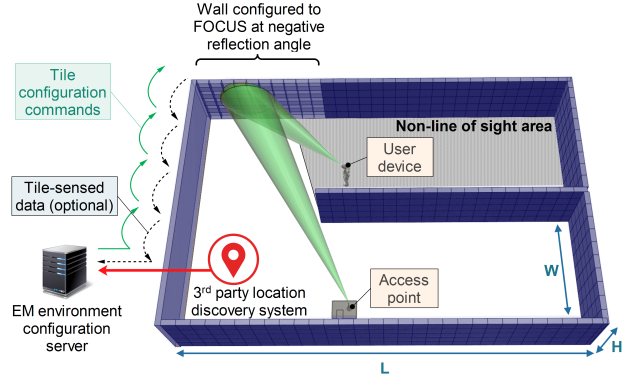


Fig. 5: Illustration of a customized wireless indoor environment. STEER functions are applied to several tiles, to achieve a FOCUS behavior of the corresponding wall as a whole.

at 10m for 60GHz , instead of 60dB for 2.4GHz), ii) acute multi-path fading even in LOS cases, iii) strong Doppler shift even at pedestrian speeds, iv) optical-like propagation of EM waves, limiting connectivity to LOS cases and exhibiting strong sensitivity to shadowing phenomena. Attenuation due to molecular absorption may not play a significant role in indoor cases—depending on the composition of the environment—as it corresponds to 10^{-5}dB/m loss [1].

Given the mentioned mm-wave considerations, we proceed to present mitigation measures offered by a HyperSurface-enabled environment. We consider the setup of Fig. 5, comprising a receiver (Rx)-transmitter (Tx) pair located in NLOS over a known floorplan. The walls are coated with HyperSurface tiles. Furthermore, we consider the existence of a location discovery service (e.g., [30]), which reports the location of the user device. At first, the Rx and Tx may attempt high-power, omni-directional communication. The location discovery service pinpoints the location of the user device and sends it to the EM environment configuration server. (Without loss of generality, the location of the Tx/access point can be considered known). Tiles may sense their impinging power and report it to the server as well. The server can use this information to increase the accuracy of the discovered user device location. Subsequently, the following actions take place:

- The tiles at the top-left part of Fig. 5 are set to a symmetric “negative focus” setup as shown.
- The Tx and the Rx are signaled to direct their antenna patterns to the configured tiles using beamforming.

Using this approach, the path loss can be even fully mitigated, since the emitted energy is focused at the communicating endpoints, rather than scattering within the environment. This can also be of benefit to the user device’s battery lifetime, given that the redundantly emitted power is minimized. Concerning multi-path fading, the fine-grained EM control over the wave propagation can have as an objective the *crafting* of a power delay profile that mitigates the phenomenon, e.g., by ensuring a path with significantly more power than any other, or one that best matches the MIMO capabilities of the devices. Additionally, the focal point of the EM wave reflected by the

tilled wall towards the use device can be altered in real-time, to match the velocity of the mobile user. Mobile trajectory predictions can be employed to facilitate this course of action. This provides a potential mitigation approach for Doppler phenomena.

The environment optimization for multiple user pairs, or sub-spaces within the environment, may be of increased practical interest. Returning to the setup of Fig. 5, the configuration server can, e.g., set the tiles to preemptively minimize the delay spread within the whole NLOS area, while ensuring a minimum level of received power within it. In the sub-space optimization case, the best matching tile configurations can be calculated offline and be deployed upon request. This approach is evaluated in Section VI.

Finally, it is noted that the programmable environment extends the communication distance of devices, without requiring extra dissipation of energy within the environment (e.g. by placing additional access points). This can constitute a considerable advantage for mm-wave communications, which are known to be highly absorbable by living tissue. Moreover, assuming tiles with state-preserving switch elements, the energy footprint of the programmable environment can be extremely low, especially in static or mildly changing user positions.

VI. EVALUATION IN 60GHz AND 2.4GHz SETUPS

We proceed to evaluate the HyperSurface potential in mitigating the path loss and multi-path fading effects, using a simulation platform. Specifically, the indoor 3D space of Fig. 5 is ported to a full-3D ray-tracing engine [31], customized to take into account HyperSurface tile functions. The evaluation focuses on finding tile configurations that optimally mitigate the path loss and multi-path fading for 12 users within the NLOS area. We study the case of 60GHz, which is of increased interest to upcoming 5G communications, as well as the 2.4GHz case due to its wide applicability, e.g., to WiFi setups [5].

Concerning the simulation parameters, the space has a height of $H = 3m$, corridor length (distance between opposite wall faces) $L = 15m$, corridor width $W = 4.5m$, a middle wall length of $12m$, and $0.5m$ wall thickness. Two stacked walls exist in the middle. The floor and ceiling are treated as plain, planar surfaces composed of concrete, without HyperSurface functionality. All walls are coated with HyperSurface tiles, which are square-sized with dimensions $1 \times 1m$. Thus, the 3D space comprises a total of 222 tiles.

The dynamic metasurface pattern of Fig. 2 is considered, using mechanical, state-preserving switches (ON/OFF states are allowed). Appropriate dimensions are assumed, for 60GHz and 2.4GHz respectively, as explained in the context of Fig. 2. This pattern design has been extensively studied in literature, offering a wide range of steering and absorbing capabilities, even with switch elements only at the horizontal direction [29, p. 235]. Although beyond of the present scope, it is noted that this metasurface design also exhibits tunable EM interaction frequency, yielding a particularly extended repertoire of supported tunability parameters. The considered tile functions account

for EM wave steering and absorption from various DoAs. Specifically, we allow for any DoA and reflection direction resulting from the combination of $\{-30^\circ, -15^\circ, 0^\circ, 15^\circ, 30^\circ\}$ in azimuth and $\{-30^\circ, -15^\circ, 0^\circ, 15^\circ, 30^\circ\}$ in elevation planes, using the tile center as the origin. Notice that the considered angles have been shown to be commonly attainable by metasurfaces [32]. However, carefully designed, static metasurfaces have achieved nearly full angle coverage, i.e., almost $(-90^\circ, 90^\circ)$ in azimuth and elevation, which is indicative of their potential [33]. The reflection coefficient is set to 100% for each steering function [29, p. 235]. Additionally, we consider an EM absorbing tile function which reduces the power of impinging waves (given DoA) by 35dB [29, p. 235], scattering the remaining wave power towards the Snell law-derived reflection direction. Thus, a tile supports 26 different function configurations in total.

Existing ray-tracing engines employ common laws of optics to simulate the propagation of waves. As such, current ray-tracers do not readily allow for custom wave steering functions. (Absorbing functions, on the other hand, are readily supported). Thus, to implement steering functions we work as follows. First, the following observation is made:

Remark 1. Assume a tile and a set of a required wave DoA and a reflection direction upon it, not abiding by Snell's law. There exists a rotation of the tile in 3D space that makes the wave DoA and reflection direction comply with Snell's law.

Based on this Remark, the custom steering functions are implemented by tuning the tile's spatial derivative as follows. Since a tile is a flat, square surface in a 3D space, its spatial derivative is normally an arrow perpendicular to the tile surface. In order to allow for custom EM wave steering within the ray-tracing engine, we allow for virtually rotating the spatial derivative (but not the tile itself) by proper azimuth and elevation angles. The modified spatial derivative is then used in all ray-tracing calculations.

The external service is considered to know the tile specifications, i.e., the tile configuration that corresponds to each virtual angle combination. The service has obtained the direction of the impinging wave at each tile via the distributed sensing elements. Subsequently, it deploys the corresponding STEER or ABSORB commands at each tile, by applying the corresponding tile configuration.

An EM transmitter (Tx) is placed at position $\{7, 12, 2\}m$ (with respect to the origin placed on the floor level, at the upper-left corner of Fig. 5). It is equipped with a half-dipole antenna and transmits at a carrier frequency of 60GHz or 2.4GHz (two studies) and 25MHz bandwidth. The transmission power is set to 100dBmW, a high number chosen to ensure that no propagation paths are disregarded by the ray-tracer due to its internal, minimum-allowed path loss threshold. The NLOS area is defined as $x \in [0, 4]m$, $y \in [0, 15]m$ and a constant height of $z = 1.5m$. Within the NLOS area, a set 12 receivers—with antennas identical to the transmitter—are placed at a regular 2×6 uniform grid deployment, with 2.5m spacing. The receiver grid is centered in the NLOS area. Intermediate

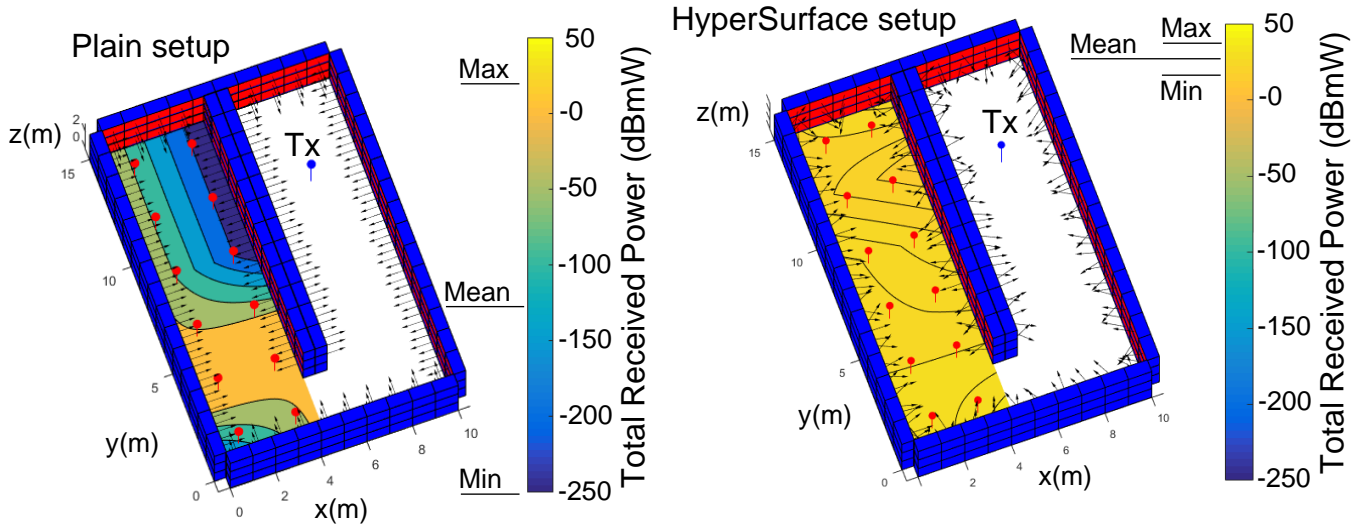


Fig. 6: Wireless environment optimization case study (A) for 60GHz and comparison to the plain case (non-HyperSurface). The objective is to maximize the minimum total received power over the NLOS area receivers (red dots).

signal reception values, used only for illustration purposes in the ensuing Figures, are produced by means of interpolation.

The evaluation scenario considers two case studies, corresponding to the path loss and multi-path fading mitigation objectives. In each case, the state of each of the 222 tiles is treated as an input variable of an appropriate objective function which must be optimized. Given the vastness and discontinuity of the solution space (i.e., 222^{26} possible tile configurations, positioned at different walls) and the discrete nature of the input variables, a Genetic Algorithm (GA) is chosen as the optimization heuristic [29], using the MATLAB Optimization Toolbox implementation [34]. GAs are heuristics that are inspired by evolutionary biology principles. They treat the variables of an optimization problem as *genomes* which compete with each other in terms of best fitness to an optimization objective. Good solutions are combined iteratively by exchanging *genes*, i.e., variable sub-parts, producing new generations of solutions. In the problem at hand, a genome represents a complete tile configuration, i.e., an array containing the state of the 222 tiles. A gene represents the state of each tile, i.e., the specific array elements. Two optimization cases are studied, denoted as (A) and (B), both for 60GHz and 2.4GHz . These are defined as follows:

- **Case study (A).** This case expresses the path loss mitigation goal, and is defined as the following optimization objective: *Define the optimal tile configurations that maximize the minimum received power over the 12 receivers in the NLOS area.*
- **Case study (B).** The case expresses the multi-path fading mitigation goal and is defined as the following optimization objective: *Define the optimal tile configurations that minimize the maximum delay spread over the 12 receivers*

TABLE I: COMPARISON OF TOTAL RECEIVED POWER (CASE A) AND POWER DELAY PROFILE (CASE B) WITH AND WITHOUT HYPERSURFACE (HSF) TILES AT 60GHz .

	Case A (dBmW)		Case B (nsec)	
	HSF setup	Plain setup	HSF setup	Plain setup
Max	34.98	22.63	0.69	3.6
Mean	25.38	-75	0.0068	0.48
Min	16.13	-250	0.0045	0.007

in the NLOS area, with the constraint of ensuring a minimum total received power (custom threshold).

For Case (B), the thresholds are set to 1dBmW for 60GHz , and 30dBmW for 2.4GHz , based on the floor-plan dimensions and the path loss levels discussed in Section V.

The results for the 60GHz case are shown in Fig. 6, 7 and are summarized in Table. I. Figure 6 presents case (A) for the plain (left) and HyperSurface-enabled (right) environments. In the plain setup, the tile spatial derivatives (black arrows) are naturally perpendicular to the tile surfaces. The average received power over the 12 NLOS area receivers is -75dBmW , while the minimum power is -250dBmW , which is the lowest level allowed by the ray-tracing engine. Thus, the bottom-left and the three top-right receivers of the NLOS area are essentially disconnected in the plain setup. The maximum total received power is 22.63dBmW .

The right inset of Fig. 6 shows the corresponding results with the HyperSurface functionality enabled. Notably, the minimum power level over the NLOS area is 16.13dB , which constitutes a raise by at least 266.13dBmW with regard to the plain case. Moreover, the received power becomes essentially uniform over the NLOS area, ranging between 16.13 and 34.98dBmW , with an average of 25.38dBmW . The tile spatial derivatives exhibit a degree of directivity towards the previously disconnected area parts (e.g., cf. left-most wall). Moreover, the top-and bottom

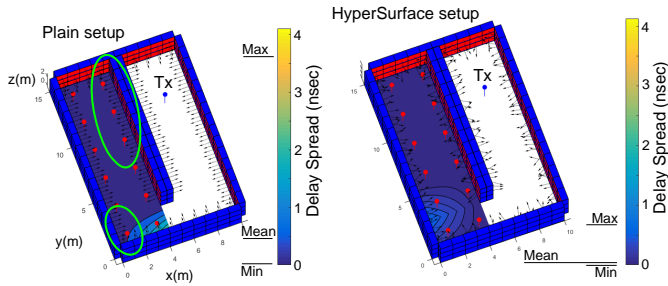


Fig. 7: Wireless environment optimization case study (B) for 60 GHz. The objective is to minimize the maximum delay spread over the NLOS area, while ensuring a minimum of 1 dBmW total received power per receiver. The circled parts of the plain setup correspond to disconnected areas. (cf. Fig. 6-left).

TABLE II: COMPARISON OF TOTAL RECEIVED POWER (CASE A) AND POWER DELAY PROFILE (CASE B) WITH AND WITHOUT HYPERSURFACE (HSF) TILES AT 2.4 GHz.

	Case A (dBmW)		Case B (nsec)	
	HSF setup	Plain setup	HSF setup	Plain setup
Max	59.81	47	0.68	3.65
Mean	51.37	-58	0.067	0.47
Min	45.13	-250	0.0029	0.0014

tiles across the height of the walls tend to focus towards the NLOS area height. The non-uniformity of the derivatives is in accordance with the nature of the Genetic Algorithm, which is a very exploratory but not gradient-ascending optimizer [35]. This means that there exists potential for an even better optimization result near the Genetic Algorithm-derived solution.

The case (B) results for 60 GHz are shown in Fig. 7. The objective is to minimize the maximum delay spread over the 12 NLOS receivers, under the constraint for at least 1 dBmW total received power per receiver. For the plain setup, shown in the left inset, we note a maximum delay spread of approximately 3.6 nsec. The 1 dBmW minimum power constraint is of course not satisfied, as previously shown in Fig. 6-left. The circled areas correspond to the under-powered/disconnected NLOS area parts. The minimum and average delay spread over the *connected* areas only are 7 psec and 0.48 nsec respectively. The HyperSurface-enabled setup (right inset), achieves 5.21 times lower maximum delay spread (0.69 nsec) than the plain setup, a minimum of 4.5 psec delay spread (1.5 times lower), and an average of 6.8 psec (70 times lower). This significant performance improvement is accompanied by considerable total power levels, in the range of [7.07, 16.93] dBmW (average: 10.64 dBmW), fulfilling the optimization constraint of 1 dBmW.

The results for the 2.4 GHz case are similar to the 60 GHz in terms of improvement, and are collectively given in Fig. 8 and Table II. The objective in the two leftmost panels is to maximize the minimum total received power over the 12 receivers in the NLOS area. The plain setup achieves -250, -58 and 47 dBmW minimum, average and maximum total received power, respectively. The HyperSurface setup yields considerably improved results, with 45.13, 51.37 and

59.81 dBmW minimum, average and maximum total received power, respectively. Thus, there is a gain of 295.13 dBmW in minimum received power.

The delay spread improvement is also significant, as shown in the two rightmost panels. The plain setup yields 1.4 psec, 0.47 nsec and 3.65 nsec minimum, average and maximum delay spread values, with 4 disconnected receivers (circled parts, cf. first inset of Fig. 8). The corresponding HyperSurface-enabled setup achieves 2.9 psec, 67 psec and 0.68 nsec min/average/max respectively. Moreover, it ensures a minimum total received power of 34.12 dBmW, successfully meeting the 30 dBmW optimization constraint.

A. Discussion

The results of Section VI demonstrated the path loss and multi-path fading mitigation potential of the proposed softwarization of wireless indoor environments. Even at the highly-challenging 60 GHz communications, a HyperSurface tile-coated indoor setup exhibited significant improvements in received power levels and delay spread. Such traits can benefit the communication distance of devices and their energy consumption, without dissipating more energy in the—already EM-strained—environments via retransmitters. This promising performance can encourage further exploration of the HyperSurface concept in additional usage domains:

Multiple applications can be studied in both indoor and outdoor environments, and in the context of multiple systems, such as 5G, IoT and D2D, where ultra-low latency, high bandwidth, and support for massive numbers of devices is important [6]. Moreover, HyperSurfaces may act as an enabler for upcoming THz communications. Operation in this band promises exceptional data rates and hardware size minimization at the nano-level, which can enable a wide range of groundbreaking applications [36]. Nonetheless, the THz band is susceptible to acute signal attenuation owed to molecular absorption. HyperSurfaces with graphene-based meta-atom designs could act as a smart environment for THz communications [37], mitigating the attenuation effects and extending the communication range.

VII. CONCLUSION

The present study proposed an indoor wireless communication paradigm where the electromagnetic propagation environment becomes aware of the ongoing communications within it. The key idea is to coat objects such as walls, doors and furniture with HyperSurface tiles, a forthcoming type of material with programmable electromagnetic behavior. HyperSurfaces can exert fine-grained control over impinging electromagnetic waves, steering them toward completely custom directions, polarizing them or fully absorbing them. HyperSurfaces have inter-networking capabilities, allowing for the first time the participation of electromagnetic properties of materials into control loops. A central server maintains a view of the communicating devices within an indoor space, and subsequently sets the tile electromagnetic configuration in accordance with any optimization objective. The HyperSurface

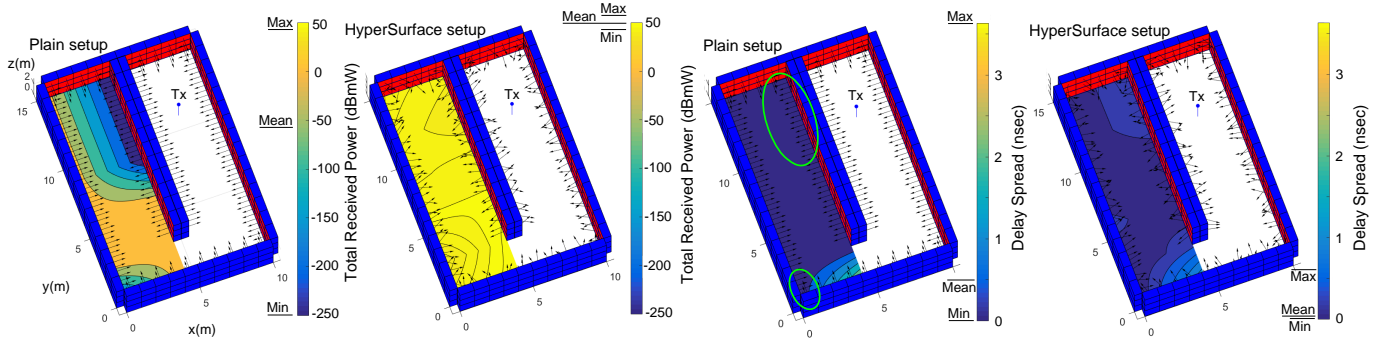


Fig. 8: Wireless environment optimization case studies (A: left-two insets) and (B: right-two insets) for the 2.4GHz case.

tile concept has been evaluated in 2.4 and 60 GHz setups, which demonstrated its high potential for path loss and multi-path fading mitigation, from microwave to mm-wave setups.

ACKNOWLEDGMENT

This work was funded by the European Union via the Horizon 2020: Future Emerging Topics call (FETOPEN), grant EU736876, project VISORSURF (<http://www.visorsurf.eu>).

The concept of Programmable Wireless Environment was introduced in the viewpoint article [2] by the respective authors.

Programmable Wireless Environments are provisionally patented by the authors of [2] as: "A New Wireless Communication Paradigm: Realizing Wireless Environments through Software-controlled Metasurfaces", US 62/539,831, filed 10-Aug-2017.

The present work has been published in conference form in [4].

A journal version of the present work appears in [3].

REFERENCES

- [1] Z. Pi, J. Choi, and R. Heath, "Millimeter-wave gigabit broadband evolution toward 5G: fixed access and backhaul," *IEEE Communications Magazine*, vol. 54, no. 4, pp. 138–144, 2016.
- [2] C. Liaskos, A. Tsioliaridou, A. Pitsillides, S. Ioannidis and I. Akyildiz, "Using any Surface to Realize a New Paradigm for Wireless Communications," *Communications of the ACM*, in press, 2018.
- [3] C. Liaskos, S. Nie, A. Tsioliaridou, A. Pitsillides, S. Ioannidis and I. Akyildiz, "A New Wireless Communication Paradigm through Software-controlled Metasurfaces," *IEEE Communications Magazine*, in press, 2018.
- [4] C. Liaskos, S. Nie, A. Tsioliaridou, A. Pitsillides, S. Ioannidis and I. Akyildiz, "Realizing Wireless Communication through Software-defined HyperSurface Environments," *IEEE Communications Magazine*, In proceedings of the 19th IEEE International Symposium on a World of Wireless, Mobile and Multimedia Networks (IEEE WoWMoM 2018), June 12-15, 2018, Chania, Greece.
- [5] T. Yilmaz and O. B. Akan, "Millimetre-Wave Communications for 5G Wireless Networks," *Opportunities in 5G Networks: A Research and Development Perspective*, pp. 425–440, 2016.
- [6] A. Aijaz, M. Simsek, M. Dohler, and G. Fettweis, "Shaping 5G for the Tactile Internet," in *5G Mobile Comm.* Springer, 2017, pp. 677–691.
- [7] J.-M. Kelif *et al.*, "A 3D beamforming analytical model for 5G wireless networks," in *14th WiOpt*, 2016, pp. 1–8.
- [8] S. V. Hum, M. Okoniewski, and R. J. Davies, "Modeling and design of electronically tunable reflectarrays," *IEEE transactions on Antennas and Propagation*, vol. 55, no. 8, pp. 2200–2210, 2007.
- [9] J. Huang, L. I. Wenxiang, Y. Su, and F. Wang, "Multi-rate combination of partial information based routing and adaptive modulation and coding for space deterministic delay/disruption tolerant networks," *IET Communications*, 2017.
- [10] S. Han and K. G. Shin, "Enhancing Wireless Performance Using Reflectors," in *INFOCOM 2017*, pp. 1–10.
- [11] Y. Chen, S. He, F. Hou, Z. Shi, and J. Chen, "Promoting device-to-device communication in cellular networks by contract-based incentive mechanisms," *IEEE Network*, vol. 31, no. 3, pp. 14–20, 2017.
- [12] A. Y. Zhu *et al.*, "Traditional and emerging materials for optical metasurfaces," *Nanophotonics*, vol. 6, no. 2, 2017.
- [13] A. E. Minovich, A. E. Miroshnichenko, A. Y. Bykov, T. V. Murzina, D. N. Neshev, and Y. S. Kivshar, "Functional and nonlinear optical metasurfaces: Optical metasurfaces," *Laser & Photonics Reviews*, vol. 9, no. 2, pp. 195–213, 2015.
- [14] S. Lucyszyn, *Advanced RF MEMS*, ser. The Cambridge RF and microwave engineering series. NY: Cambridge Univ. Press, 2010.
- [15] H.-T. Chen, A. J. Taylor, and N. Yu, "A review of metasurfaces: physics and applications," *Reports on progress in physics. Physical Society (Great Britain)*, vol. 79, no. 7, p. 076401, 2016.
- [16] S. H. Lee *et al.*, "Switching terahertz waves with gate-controlled active graphene metamaterials," *Nature Materials*, vol. 11, no. 11, pp. 936–941, 2012.
- [17] B. Banerjee, *An introduction to metamaterials and waves in composites*. Boca Raton, FL: CRC Press/Taylor & Francis Group, 2011.
- [18] K. Iwaszczuk *et al.*, "Flexible metamaterial absorbers for stealth applications at terahertz frequencies," *Optics Express*, vol. 20, no. 1, p. 635, 2012.
- [19] R. J. Mailloux, *Phased array antenna handbook*. Artech House Boston, 2005, vol. 2.
- [20] H. Yang, X. Cao, F. Yang, J. Gao, S. Xu, M. Li, X. Chen, Y. Zhao, Y. Zheng, and S. Li, "A programmable metasurface with dynamic polarization, scattering and focusing control," *Scientific reports*, vol. 6, p. 35692, 2016.
- [21] PCBcart. (2017) Printed circuit board calculator. [Online]. Available: <https://www.pcbcart.com/quote>
- [22] M. Caironi, *Large area and flexible electronics*. John Wiley & Sons, 2015.
- [23] M. A. U. Karim, S. Chung, E. Alon, and V. Subramanian, "Fully inkjet-printed stress-tolerant microelectromechanical reed relays for large-area electronics," *Advanced Electronic Materials*, vol. 2, no. 5, 2016.
- [24] R. Parashkov, E. Becker, T. Riedl, H.-H. Johannes, and W. Kowalsky, "Large area electronics using printing methods," *Proceedings of the IEEE*, vol. 93, no. 7, pp. 1321–1329, 2005.
- [25] I. F. Akyildiz *et al.*, "NanonetWORKS: A new communication paradigm," *Computer Networks*, vol. 52, no. 12, pp. 2260–2279, 2008.
- [26] J. E. Hopcroft, R. Motwani, and J. D. Ullman, *Automata theory, languages, and computation*, 2006, vol. 24.
- [27] C. Verikoukis *et al.*, "Internet of Things: Part 2," *IEEE Communications Magazine*, vol. 55, no. 2, pp. 114–115, 2017.
- [28] C. L. Holloway *et al.*, "An Overview of the Theory and Applications of Metasurfaces: The Two-Dimensional Equivalents of Metamaterials," *IEEE Antennas and Propagation Magazine*, vol. 54, no. 2, pp. 10–35, 2012.
- [29] R. L. Haupt and D. H. Werner, *Genetic algorithms in electromagnetics*. John Wiley & Sons, 2007.
- [30] J. Chen *et al.*, "Pseudo lateration: Millimeter-wave localization using a single rf chain," in *Wireless Communications and Networking Conference (IEE WCNC)*, 2017, pp. 1–6.

- [31] Actix Ltd, "Radiowave Propagation Simulator SE," <http://actix.com>, 2010.
- [32] M. Yazdi and M. Albooyeh, "Analysis of Metasurfaces at Oblique Incidence," *IEEE Transactions on Antennas and Propagation*, vol. 65, no. 5, pp. 2397–2404, 2017.
- [33] M. Albooyeh *et al.*, "Resonant metasurfaces at oblique incidence: interplay of order and disorder," *Scientific reports*, vol. 4, p. 4484, 2014.
- [34] Mathworks. (2017) Genetic algorithm: Finding global optima for highly nonlinear problems. [Online]. Available: <https://www.mathworks.com/discovery/genetic-algorithm.html>
- [35] S. Luke, *Essentials of metaheuristics*, 1st ed. [S.l.]: Lulu, 2009.
- [36] I. F. Akyildiz, M. Pierobon, S. Balasubramaniam, and Y. Koucheryavy, "The internet of bio-nano things," *IEEE Communications Magazine*, vol. 53, no. 3, pp. 32–40, 2015.
- [37] K. Fan *et al.*, "Optically Tunable Terahertz Metamaterials on Highly Flexible Substrates," *IEEE Transactions on Terahertz Science and Technology*, vol. 3, no. 6, pp. 702–708, 2013.